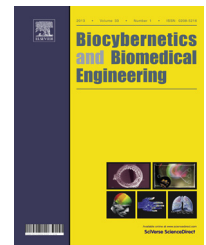




Available online at www.sciencedirect.com

ScienceDirect

journal homepage: www.elsevier.com/locate/bbe



Original Research Article

Ensemble of classifiers and wavelet transformation for improved recognition of Fuhrman grading in clear-cell renal carcinoma



Michał Kruk^a, Jarosław Kurek^a, Stanisław Osowski^{b,c,*}, Robert Koktysz^d,
Bartosz Swiderski^a, Tomasz Markiewicz^{b,d}

^a Warsaw University of Life Sciences, Warsaw, Poland

^b Warsaw University of Technology, Warsaw, Poland

^c Military University of Technology, Warsaw, Poland

^d Military Institute of Medicine, Warsaw, Poland

ARTICLE INFO

Article history:

Received 1 December 2016

Received in revised form

21 March 2017

Accepted 20 April 2017

Available online 1 May 2017

Keywords:

Ensemble of classifiers

Feature selection

Fuhrman grading

Wavelets

SVM

Random forest

ABSTRACT

The paper presents an improved system to recognition of Fuhrman grading in clear-cell renal carcinoma using an ensemble of classifiers. The novelty of solution includes the segmentation applying wavelet transformation in preprocessing stage, application of few selection methods for feature generation and using the ensemble of classifiers in final recognition step. The wavelet transformation is a very efficient tool for image de-noising and enhancing the edges of cell nuclei. The important distinction to other approaches is that diagnostic features of nuclei, based on the texture, geometry, color and histogram, are selected by using few methods, each relying on different mechanism of selection. These different sets of features have enabled creating the ensemble of classifiers based on the support vector machine and random forest, both cooperating with them. Such approach has led to the significant increase of the quality factors in comparison to the best existing results: sensitivity (the average of this solution 94.3% compared to 91.5%) and specificity (the average 98.6% compared to 97.5%).

© 2017 Published by Elsevier B.V. on behalf of Nalecz Institute of Biocybernetics and Biomedical Engineering of the Polish Academy of Sciences.

1. Introduction

A clear-cell renal carcinoma (CC-RCC) is expressed in a form of the nested tumor cells, separated from the others by the network of delicate sinusoidal vascular channels [1–4]. The

nuclear Fuhrman grading system [5] is commonly used in classifying the grades of CC-RCC. It has 4 scales, where 1 represents the best prognosis and scale 4 the worst. The grading takes into account such features as the size, shape, chromatin pattern, and also the size of nucleoli. The details of it can be found in the works [4,6–8].

* Corresponding author at: Warsaw University of Technology, 00-661 Warsaw, Koszykowa 75, Poland.

E-mail address: sto@iem.pw.edu.pl (S. Osowski).

<http://dx.doi.org/10.1016/j.bbe.2017.04.005>

0208-5216/© 2017 Published by Elsevier B.V. on behalf of Nalecz Institute of Biocybernetics and Biomedical Engineering of the Polish Academy of Sciences.

However, the manual recognition of Fuhrman grade is tedious and prone to errors. There are only small number of works devoted to the computer methods to make the solution automatic. One example of it is discussed in the papers [9,10] where the mathematical morphology in combination gradient were used to separate nuclei and the support vector machine (SVM) classifier used in final recognition of the cells. The paper [11] has shown that automatic analysis of slides allows pathologists to see the spatial distribution of nuclei size, which can be used to differentiate low-grade and high-grade clear cell RCC with good sensitivity and specificity. The paper [7] has presented the clinical decision support system for automated Fuhrman grading of renal carcinoma biopsy images, taking into account the semantic interpretation of the imaging features. The accuracy reported by authors is 90.4% in a four-class recognition. Some works presenting the application of artificial intelligence methods to the recognition of cells in chosen pathological cases, like hepatocellular carcinoma (HCC) [11] or the colon cells [12] have been also reported. There are also some works developing the universal platform able to perform the analysis of different types of microscopic images in pathological cases [13]. However, the analysis methods are specialized in particular pathologies. This is important, since each pathology type has its own specific nature and needs developing special methods of data processing.

The aim of this paper is to develop an automatic system which is able to improve the accuracy of Fuhrman grading of renal cells to the value acceptable in the medical practice, where up to 10% discrepancy of numerical results of few experts are observed. The work is an improvement of the previous solution presented in [9,10]. The novelties introduced in this paper include: application of wavelet and watershed transformation in the process of segmentation of the cells in the image, introduction of few feature selection methods and application of an ensemble of classifiers in the final stage of cell recognition. The wavelet transformation reduces the noise of the image and enhances the edges of cells, which lead to more accurate recognition of nuclei. The cells are represented here by the numerical descriptors (diagnostic features) based on the texture, geometry, color and histogram.

The important novelty is application of few selection methods used to choose the most important sets of these descriptors. Application of few feature selection procedures has allowed to analyze importance of diagnostic features from different points of view. Thanks to this step it was possible to select 5 different sets of optimal features, applied next as the input attributes for the ensemble of classifiers.

The ensemble of classifiers is able to improve the performance of a single (even the best) classifier [14]. The developed ensemble is formed on the basis of two classifiers, actually known as the best: the support vector machine (SVM) and random forest (RF), both cooperating with the selected, different sets of features. Such solution leads to better accuracy of recognition of cells and improvement of Fuhrman grading. The results of experiments presented in Table 3 show significant improvement of the performance of the system. Two types of ensemble have been developed: ensemble composed of the results of all single classifiers and ensemble taking into account only the best solutions.

The numerical results obtained thanks to these changes in data processing are much better in comparison to the original paper in AQCH or the presentation at VIPIMAGE conference. This was stressed in Tables 4 and 5.

2. Materials

The numerical experiments have been performed using the CC-RCC database created in the Military Institute of Medicine, Warsaw, Poland. Seventy patients suffering from CC-RCC were first evaluated by the medical experts and then used only in the learning phase of the system. The other sixty-two different patients, also representing all grades of the illness were used in verification of the established system. 94 randomly selected images corresponding to these patients have been analyzed.

The images of the tumor area representing the neoplasm cells of kidneys have been created using hematoxylin and eosin (H&E) staining. They were registered at magnification of 400× using an Olympus BX-61 microscope and Olympus DP-72 camera in RGB format and at 2070 × 1548 resolution. Typically one slide per patient is prepared and assessed by the expert pathologist. The number of cells representing each grade should be in the range of hundreds.

The regions of interest (ROI) in the slide, subject to further analysis, have been selected by three independent experts. Due to some natural diversity among their verdicts, following from the individual way of assessment of cells, we have decided to use only these histological slides which were assessed in the same way by all experts. Thanks to this the target value for each cell used in classification is unique and may be objectively compared to the result of our computerized system.

All ROI images were processed to get the segmentation of the individual cells. In this way the database of 3446 microscopic images of nuclei, extracted from these slides, has been created and annotated by the experts. The cells represent all Fuhrman grades (link to nuclei: <http://michalkruk.pl/FDataset.zip> and link to images before segmentation: <http://michalkruk.pl/Images.zip>). The number of cells representing the succeeding Fuhrman grades, treated in further experiments as classes, are shown in Table 1.

3. Methods

The system of Fuhrman grading developed in this paper is composed of four main steps: (1) segmentation of the individual nuclei from the H&E images, (2) definition of the numerical descriptors representing the extracted nuclei, (3) evaluation and selection of descriptors as the diagnostic features by using few selection methods and (4) application of

Table 1 – The number of cells of different grades used in experiments.

Fuhrman grade	1	2	3	4
Number of cells	1164	1133	786	363

an ensemble of the SVM and RF classifiers to recognize Fuhrman grade of the cells.

3.1. Algorithm of nuclei segmentation

The aim of segmentation is to localize the nuclei of cells in the analyzed image. Many different methods have been applied in segmentation. Among them are: linear filters used for edge detection [15], thresholding procedure [16], clusterization [17], region growing methods [18], etc. In this work the watershed transform based on the immersion simulation [16,19], combined with the wavelet transformation have been applied. The wavelet transformation [20] is used in denoising the image and enhancing the edges using multiple resolution of the image. Such technique is superior to standard denoising approaches applying usually the linear filters, like Canny, Prewitt, Hough or Laplacian [21]. Thanks to such approach the enhanced version of the image gradient [22] can be obtained. The watershed transform is performed on the gradient of the denoised and enhanced image.

The wavelet transformation is the preprocessing step of the image. Only two detail sub-images: horizontal and vertical have been used. They represent the local differences along x and y coordinates and provide good approximations for the local image gradients at different scales. Thanks to them the enhancement of the edges of the objects existing in the image has been achieved. Denoising has been obtained in a few steps [22]: 1) analysis of the image gradients with acceptance of only these points, which are above some threshold level (gradients of noise are usually smaller than these related to edges), 2) comparison of the adjacent scales of the wavelet decomposition accepting only these which last longer and 3) analysis of spatial distribution of the gradient removing the isolated points. The Daubechies wavelet db4 at four levels of decomposition has been applied in experiments [20].

The watershed implementation [16,19] is done in the next step on the wavelet preprocessed gradient image. This procedure creates the dams separating different regions of the image representing the individual cells. A post-processing stage is used to merge regions characterized by low contrast borders, to remove over-segmented regions which have too small areas and also to remove these, which don't satisfy the additional specific criteria defined by the user.

Fig. 1 presents the results of application of this segmentation process to the microscopic images of kidney tissue in H&E staining representing grades 2, 3 and 4. Left column depicts the original images, the middle one – the segmentation results obtained without application of wavelets and the right column – the results of segmentation of the same images with application of the wavelet transformation. It is evident, that application of wavelet preprocessing has improved the quality of segmentation results (better separation of close objects, more accurate representation of the nuclei shape and less noisy object area).

To make some statistical comparison 10 ROI images selected from the slides (around 100 cells) have been analyzed by our segmentation process. This analysis has confirmed good quality of solution. The population of segmented cells agreed in 98% with the expert recognition. The agreement of the shape with the expert results was also very good (average

95% after wavelet transformation, compared to 89% before its application.

3.2. Numerical descriptors of nuclei

The segmented nuclei should be described by the numerical descriptors. To obtain the highest possible diversity of image descriptors different principles of their generation have been applied. In this work the texture, morphometry, color and histogram descriptions have been applied.

Haralick descriptors refer to the texture [23,24]. 13 statistical descriptors have been used: energy, contrast, correlation, sum of variances, inverse difference moment, entropy, information measures of correlation, sum average, sum entropy, sum variance, difference variance, contrast, and difference entropy. Additionally four texture descriptors related to heterogeneity, homogeneity, clump and condensation [25] have been also defined.

The next set of morphometric features are defined for description of the geometry of nuclei. They include: the area, major axis length, minor axis length, perimeter, convex area, eccentricity equivalent diameter $ed = \sqrt{\frac{4 \cdot \text{area}}{\pi}}$ and solidity defined as the ratio of area to convex area.

Three descriptors have been defined on the basis of color. At notation of intensity of pixels corresponding to red (R), green (G) and blue (B) color components these descriptors are defined as follows $S_G = \frac{G}{R+G+B}$, $S_B = \frac{B}{R+G+B}$ and $S_R = \frac{R}{R+G+B}$. The histogram of gray representation of the nuclei image has been also used in definition of descriptors. The mean, standard deviation and kurtosis of histogram have been included as the additional set of descriptors.

The total number of descriptors defined in this way is 31. However, not all of them possess good class discrimination ability. Therefore the selection of the most important features is needed.

3.3. Selection of class discriminative features

Many methods of feature selection have been already defined. The most popular are: the principal component analysis, the correlation among features, correlation between the features and the classes, feature ranking by applying the linear or nonlinear SVM, the mean and variance of the features belonging to different classes combined into common quality measure, genetic algorithm, binary particle swarm optimization, random forest, etc. [17,26–28]. Each method selects the specific set of the most important features. To diversify the characterization of the image few selection algorithms have been applied. They include: Fisher method, genetic algorithm, random forest, correlation feature selection and fast correlation based filter.

Fisher measure of quality is based on the standard deviation and mean value of the feature describing the cells of the same class [17]. The discrimination coefficient $S_{AB}(f)$ defined for the feature f in recognition of samples belonging to classes A and B is defined in the way

$$S_{AB}(f) = \frac{|c_A(f) - c_B(f)|}{\sigma_A(f) + \sigma_B(f)} \quad (1)$$

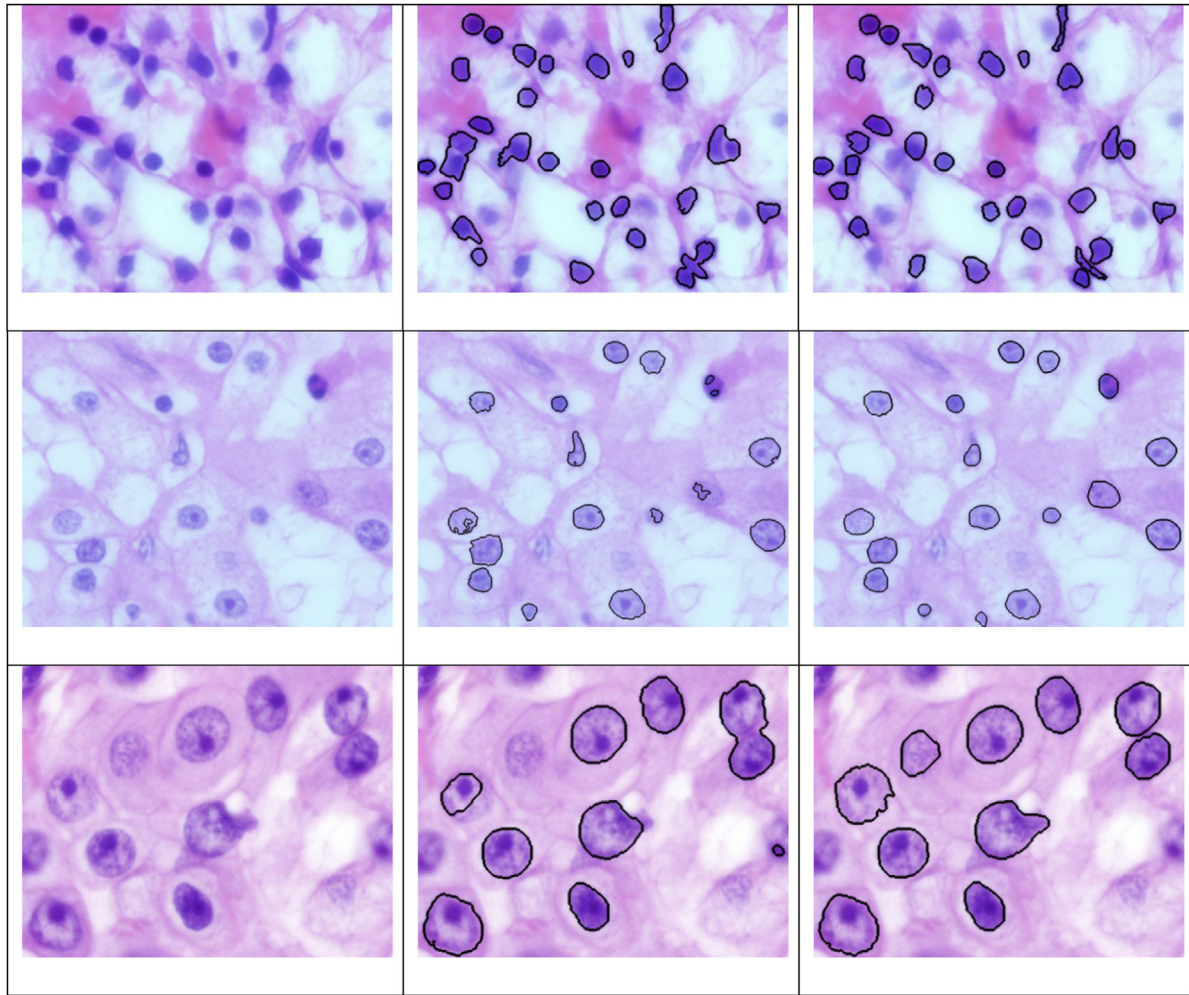


Fig. 1 – The graphical illustration of the segmentation of the H&E image of kidney tissue: left column – the original images, middle column – the segmentation results without wavelet transformation, right column - the result after application of the wavelet enhancement of the image. The majority cells in the upper row represent grade 2, in the middle row – grade 3 and in the bottom row – grade 4).

where c_A and c_B are the mean values of the feature f in the class A and B , respectively, and σ_A and σ_B the corresponding standard deviations. Good feature should have large value of the Fisher measure.

GA is a solution of global optimization. It operates with many populations of solution (called chromosomes) and applies the operations of selection of parents for reproduction, crossover, creation of the offspring and application of mutation to some bits representing the children [29]. The genetic population applied in the experiments was equal 100 chromosomes, crossover rate 80% and mutation rate 1%.

The binary chromosomes used in genetic operations are associated with the corresponding input vectors \mathbf{x} which represents the input attributes for the SVM classifier of Gaussian kernel. The value 1 in chromosome means inclusion of the feature in the vector \mathbf{x} and zero – exclusion. The learning data for classifier is created from 60% of the total data set, and the remaining 40% represent the validation data. The successively performed genetic operations lead to the minimum of the objective function defined as the error of

classification. The features corresponding to the minimum of the validation error represent the optimal set.

The random forest is also used for assessing the significance of the features in the class recognition [15,30]. The importance of feature is measured by permuting its values and assessing the increase of the classification error in comparison to original value of feature [30]. The higher is the increase of the average error the better class discrimination ability of the feature. The final number of features has been estimated by trying different number of the best features in the classification procedure and accepting this one, which provides the highest accuracy of the system on the validation data.

The next feature selection method applied in the work is the correlation feature selection (CFS) [27]. It is based on the fact, that good feature set should be well correlated with the predicted class, while the individual features should not be correlated among each other. The total measure R_{cf} of the significance of the feature set with respect to the class c is estimated in the form [27]

$$R_{cf} = \frac{NR_{ci}}{\sqrt{N + N(N-1)R_{ii}}} \quad (2)$$

The parameter N is the number of features in the set, $\overline{R_{ci}}$ is the average value of the Pearson's correlation coefficients of the analyzed set of features and the class c , while $\overline{R_{ii}}$ is the average inter-correlation between features in the set. The set of features providing the highest value of R_{cf} is treated as the best one in the classification process.

The fifth selection method used in our solution is fast correlation based filter (FCBF) [28]. It is based on the entropy, defined for the individual feature f_i and for the same feature after taking into account also another feature f_j . The method selects the set of the features significant in the class recognition process and not redundant to any of the features existing in the set.

The relevance of the feature f is estimated by defining the symmetrical uncertainty $SU(f,c)$ value for the feature f and the class c as well as all values of the measure $SU(f_i,f_j)$ for the pairwise correlations of the features [23,28]. In our experiments the threshold values for $SU(f,c) = 0.68$ and $SU(f_i,f_j) = 0.50$, selected after some introductory experiments, have been selected.

3.4. Classification system

The applied selection methods, based on various principles of operation, result in different content of the sets of features, treated by the particular methods as the best in classification process. To obtain the highest efficiency of class recognition we have applied all these sets as the input attributes to the classifiers, forming an ensemble. The ensemble is able to improve the performance of the classification system if the individual classifiers are independent in action. Different methods of achieving this independence are known and used in practice [31,32]. To get the most diversified solution of the classification problem and provide the maximum independence of the ensemble members, two types of classifiers have been used in this work: SVM [33] and RF [30]. These two well-known classification systems have been chosen because they apply different mechanisms of taking decision and at the same time have very good reputation in pattern recognition.

The SVM of Gaussian kernel function $K(\mathbf{x}, \mathbf{x}_i)$ [33] was applied in this work. The learning task of SVM is to separate the vectors \mathbf{x}_i into opposite classes with the maximum separation margin between classes. The hyperparameters in the form of the regularization constant C and Gaussian kernel width have been set by repeating the learning experiments for the set of their predefined values and accepting this one, which results in the minimum error on the validation data set. To recognize four classes of data, six 2-class recognizing SVM networks working in one-against-one mode of operation were used.

The Breiman random forest is the second classification unit used in this work [30]. It constructs many decision trees in training and responses with the class label achieving the majority among the members in an ensemble. To improve the generalization property the learning data are chosen randomly. At the same time the limited set of randomly

chosen features in each splitting node of the trees have been applied. Both RF and SVM belong to the very high efficiency classification systems.

Both classifiers were associated with the particular sets of diagnostic features chosen by five applied selection methods. In this way the ensemble composed of maximum 10 members was created (each classifier combined with the individual set of features selected by every one of the selection methods).

Fusion of the classification results of individual members of the ensemble was performed by using the random forest as an integrator. The input attributes to such integrator are formed from the output signals of the classifiers forming an ensemble. The majority of decision trees of RF are responsible for generating the final class recognition. The numerical experiments (recognition of data samples by the individual classifiers and integration of their results) are done in the 10-fold cross validation way.

4. Results of numerical experiments

The numerical experiments have been done using the samples representing all Fuhrman grades, as presented in Table 1. They were exactly the same as used in [9]. The data set was split into two independent parts to separate the stage of feature extraction from the classification. Seventy patients suffering from the CC-RCC were used only in the definition of the sets of diagnostic features. The features forming these sets were used in the classification phase of experiments, which was performed on the separate data set formed by other sixty-two patients representing also all grades of the illness. The classification stage (learning and testing) was done in 10-fold cross validation mode.

The numerical descriptors created according to the presented approach were subject to the selection using five methods. Because each method was based on different principle of operation, their results were also differing.

Table 2 presents the population of the sets of features treated by the particular method as an optimal. The following notations have been used in this table: FM – Fisher selection, GA – genetic algorithm selection, RF – random forest selection, CFS – correlation feature selection and FCBF – fast correlation based filter selection method.

Some of the features have appeared in all these sets. To such features belong: energy, contrast, correlation, area, major axis length, convex area, mean of histogram, heterogeneity, homogeneity, clump and condensation. They will be treated as the most specific descriptors in an automatic system of Fuhrman grade recognition of CC-RCC.

However, there are visible differences of class discrimination ability among these commonly selected features. Fig. 2 shows the Fisher discriminant values corresponding to them. The numbers in horizontal axis indicate the succeeding features mentioned above, i.e., 1 – energy, 2 – contrast, 3 – correlation, etc. and the vertical axis the values of their Fisher discrimination coefficient. It seems that the major axis length is the most class discriminative. Close to it are contrast, area, convex area and mean of histogram.

Most of the commonly selected features represent unintuitive values from the manual point of view performed by the

Table 2 – The size of the optimal feature sets selected by the particular methods.

Method of selection	FM	GA	RF	CFS	FCBF
Number of features	19	14	19	22	17

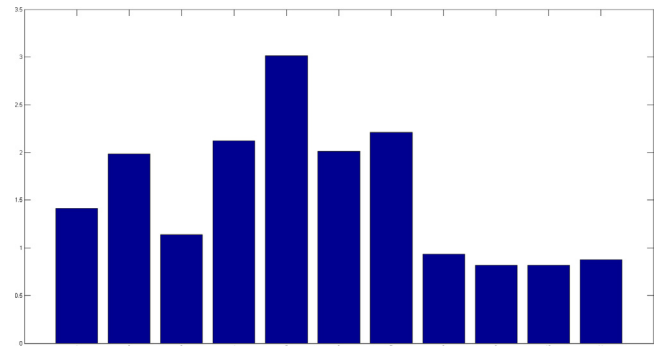
human expert. However, some of them indicate which easily accessible descriptors are important in manual assessment of the slides. To such elements belong for example area, convex area, major axis length or histogram.

In the next step these five feature sets have been used as the input attributes to the SVM and RF classifiers in the classification stage. Ten members of the classifier ensemble have been created in this way. The classifiers have generated their own outputs, which were subject to fusion into the final verdict by using the random forest as an integrating unit. The SVM and RF classifiers are known as a solutions relatively tolerant to the small population size of the samples used in learning. The number of samples representing all families of cells (above 300) were sufficient to make the objective assessment of the classification system.

All classification experiments have been performed in the 10-fold cross validation mode. The available data set was split randomly into 10 equal parts. Nine of them were used in learning the classification system and one used only in the testing. The learning and testing phases have been repeated 10 times, each time changing the testing subset. The final testing error is estimated as the average of the testing errors committed by the system in all 10 runs.

Table 3 shows the statistical results of testing the individual classifiers and their integrated output. They represent the accuracy of recognition of the particular Fuhrman grade obtained by the individual classifiers, ensemble composed of all classifiers, called full ensemble (FE) and the limited ensemble (LE) created from the most accurate classifiers in learning mode: (SVM + FM, SVM + RF, RF + RF, RF + FCBF). The limited ensemble fusing the best individual classifiers has appeared the most successful.

Its results were superior to all individual classifiers and slightly better than full ensemble (FE) composed of all classifiers. For this best solution the confusion matrix has

**Fig. 2 – Fisher discriminant values of the commonly selected features.**

been created. It is represented in Table 4. The diagonal elements depict the number of correctly recognized classes and the off-diagonal elements – the misclassifications.

On the basis of this matrix the sensitivity and specificity of the system (the last two columns) have been calculated. The average accuracy of classification achieved in experiments was equal 96.7%. The obtained results of sensitivity and specificity have been compared to the previous best results presented in [9] for the same database. They are depicted in Table 5.

The accuracy of the best previous solution [9] was 93.1%. It is significantly worse than 96.7% achieved now. In respect of all quality measures (accuracy, sensitivity and specificity) the improved system performed much better than the best previous one

The additional experiments have been performed using only 11 features selected commonly by all selection methods (Table 6). However, the results were inferior to the best obtained by the limited ensemble. On the other hand, removing some highest rank features from the selected sets, immediately led to decreasing the quality factors of the class recognition.

These results prove, that the best features used in machine learning fulfill the most important role, however, the less

Table 3 – The accuracy of Fuhrman grade recognition of the classification system in 10-fold cross validation mode.

Classifier	SVM + FM	SVM + GA	SVM + RF	SVM + CFS	SVM + FCBF	RF + FM	RF + GA	RF + RF	RF + CFS	RF + FCBF	FE	LE
Grade 1	0.978	0.967	0.981	0.952	0.971	0.975	0.965	0.975	0.947	0.972	0.974	0.981
Grade 2	0.951	0.947	0.962	0.925	0.948	0.950	0.943	0.973	0.932	0.941	0.943	0.976
Grade 3	0.922	0.898	0.931	0.911	0.918	0.919	0.898	0.943	0.926	0.914	0.917	0.943
Grade 4	0.861	0.859	0.867	0.843	0.860	0.860	0.857	0.858	0.847	0.860	0.854	0.874

Table 4 – The confusion matrix corresponding to Fuhrman grade recognition by an ensemble.

	Grade 1	Grade 2	Grade 3	Grade 4	Sensitivity	Specificity
Grade 1	1142	16	6	0	98.1%	98.9%
Grade 2	12	1106	14	1	97.6%	98.1%
Grade 3	8	17	740	21	94.1%	98.0%
Grade 4	3	11	32	317	87.3%	99.3%

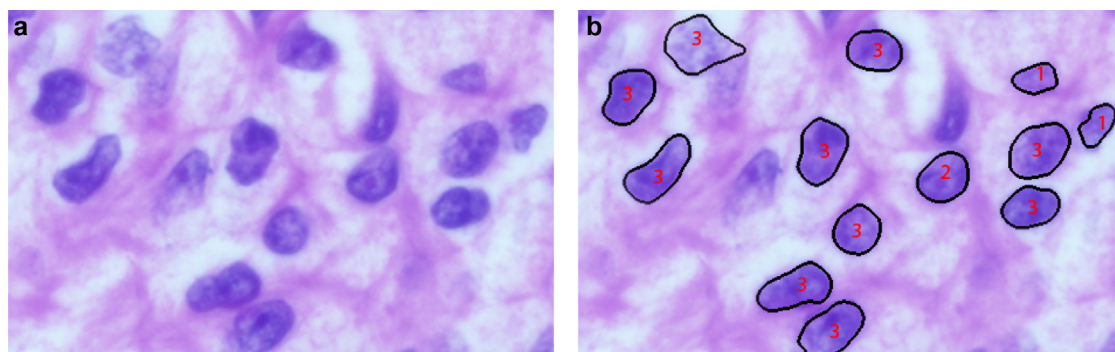


Fig. 3 – The image of clear-cell renal carcinoma subject to the analysis: a) the original image of ROI, b) the ROI image with recognized and annotated cells.

Table 5 – Comparison of the obtained class sensitivity and specificity in recognition of the Fuhrman grade of the cells.

Fuhrman grade	Grade 1	Grade 2	Grade 3	Grade 4
Actual sensitivity	98.1%	97.6%	94.1%	87.3%
Previous best sensitivity	96.7%	94.2%	91.6%	84.3%
Actual specificity	98.9%	98.1%	98.0%	99.3%
Previous best specificity	98.2%	95.7%	97.4%	98.7%

Table 6 – The accuracy results of grade recognition using only 11 features chosen commonly by all selection methods.

Classifier	Grade 1	Grade 2	Grade 3	Grade 4
SVM	0.961	0.932	0.901	0.852
RF	0.957	0.929	0.897	0.847

important features are also needed to enhance the information of the problem. This is in concordance with the well-known fact from genetic theory, that worse fit parents mixed with these of highest fit may lead to the better off-springs.

The developed approach allows also presenting the results in a graphical form, which might be very useful in visual verification of analysis results made by the medical expert. Fig. 3a presents the original image, which was subject to the analysis and Fig. 3b its automatically annotated result presenting the recognized classes of cells. The cells have been annotated in numerical way, where 1 refers to Fuhrman grade 1, 2 to grade 2 etc.

5. Conclusions

The paper has presented the improved method of Fuhrman grading recognition in clear-cell renal carcinoma. The significant modifications have been introduced in cell segmentation, feature selection and classification system. The accuracy of the image segmentation has been significantly increased by applying the wavelet transformation. Thanks to it the enhancements of the edges of the cells as well as effect of denoising the image have been achieved. Better, more

accurate identification of cell nuclei has been obtained in this way.

The important step in improvement of the quality of the cell recognition system is application of few feature selection methods: genetic algorithm, random forest, CFS, FCBF and Fisher measure. Parallel, independent application of them has allowed estimating significance of the numerical descriptors using different mechanism of assessment.

The additional advantage of different selection methods was creating the base for ensemble of classifiers. The diagnostic features chosen by the particular methods have been associated with two efficient classification systems: SVM and RF, integrated into the final system of cell recognition. The quality factors of such classification system (accuracy, sensitivity and specificity) resulting from such integration are significantly better than these obtained from the single recognizing unit. The numerical results have confirmed the increased values of these parameters.

The developed automatic system is characterized by the repeatability of results in many runs. This is not the case for the human expert results, which are dependent on the expert and his/her mental or physical disposition in the time of image analysis. Moreover, the computer system reduces the computation time required for the image analysis in comparison to the time needed by the human expert.

The study presented here will be developed in few directions. First, the experiments performed on larger data base (more patient, more cells) should be done to obtain more objective assessment of the method. There is also need to increase the number of numerical descriptors and selection methods. The additional work should be done to find automatically the regions of interest in the analyzed images. This is an important task to make system fully automatic.

REFERENCES

- [1] Kontak JA, Campbell SC. Prognostic factors in renal cell carcinoma. *Med Biol Eng Comput* 2003;30:467–80.
- [2] Bostwick DG, Cheng L. *Urologic surgical pathology*. Philadelphia: Mosby Elsevier; 2008.
- [3] Perroud B, Ishimaru T, Borowsky AD, Weiss RH. Grade-dependent proteomics characterization of kidney cancer. *Mol Cell Proteomics* 2009;8:971–85.

- [4] Delahunt B. Advances and controversies in grading and staging of renal cell carcinoma. *Modern Pathol* 2009;22:24–36.
- [5] Fuhrman SA, Lasky LC, Limas C. Prognostic significance of morphologic parameters in renal cell carcinoma. *Am J Surg Pathol* 1982;6:655–63.
- [6] Yeh FC, Parwani AV, Pantanowitz L, Ho C. Automated grading of renal cell carcinoma using whole slide imaging. *J Pathol Inform* 2014;5:23.
- [7] Champion A, Lu G, Walker M, Kothari S, Osunkoya AO, Wang MD. Semantic interpretation of robust imaging features for Fuhrman grading of renal carcinoma. *Proc. Conf. IEEE Eng Med. Biol. Soc.*. 2014. pp. 6446–9.
- [8] Chrom P, Stec R, Semeniuk-Wojtas A, Bodnar L, Spencer NJ, Szczyluk C. Fuhrman grade and neutrophil-to-lymphocyte ratio influence on survival in patients with metastatic renal cell carcinoma treated with first-line tyrosine kinase inhibitors. *Clin Genitourinary Cancer* 2016;14:457–64.
- [9] Kruk M, Osowski S, Markiewicz T, Słodkowska J, Koktysz R, Kozłowski W, et al. Computer approach to recognition of Fuhrman grade of cells in clear-cell renal cell carcinoma. *Analyt Quant Cytol Histol* 2014;36(3):147–60.
- [10] Kruk M, Kurek J, Osowski S, Koktysz R. Improved computer recognition of Fuhrman grading system in analysis of clear-cell renal carcinoma. *Proc. VIPIMAGE Conf., Canary Islands*. 2015. pp. 221–6 (printed CRC Press/Balkema).
- [11] Huang PW, Lai YH. Effective segmentation classification for HCC biopsy images. *J Pattern Recognition* 2010;43:1550–63.
- [12] Kruk M, Osowski S, Koktysz R. Recognition and classification of colon cells applying the ensemble of classifiers. *Comput Biol Med* 2009;39:156–65.
- [13] Markiewicz T, Korzynska A, Kowalski A, Swiderska-Chadaj Z, Murawski P, Grala B, et al. MIAP – Web-based platform for the computer analysis of microscopic images to support the pathological diagnosis. *Biocybernet Biomed Eng* 2016;36(4):597–609.
- [14] Nanni L, Brahnam S, Ghidoni S, Lumini A. Toward a general-purpose heterogeneous ensemble for pattern classification. *Comput Intell Neurosci* 2015. <http://dx.doi.org/10.1155/2015/909123>
- [15] Matlab user manual – Image processing toolbox. Natick: MathWorks; 2015.
- [16] Soille P. *Morphological Image Analysis, Principles applications*. Berlin: Springer; 2003.
- [17] Tan PN, Steinbach M, Kumar V. *Introduction to data mining*. Boston: Pearson Education Inc.; 2006.
- [18] Mubarak DM, Sathik MM, Beevi SZ, Revathy K. A hybrid region growing algorithm for medical image segmentation. *Int J Comp Sci Inf Technol* 2012;4(3):61–70.
- [19] Luc V, Soille P. Watersheds in digital spaces: an efficient algorithm based on immersion simulation. *IEEE Trans Pattern Anal Mach Intell* 1991;13(6):583–98.
- [20] Daubechies I. *Ten lectures on wavelets*. Philadelphia: SIAM; 1992.
- [21] Gonzalez RC, Woods RE. *Digital Image Processing*. second ed. Prentice Hall; 2002.
- [22] Jung CR, Scharcanski J. Robust watershed segmentation using wavelets. *Image Vision Comput* 2005;23:661–9.
- [23] Wagner T. Texture analysis. In: Jahne B, Haussecker H, Geisser P, editors. *Book of Computer Vision Application*. Boston: Academic Press; 1999 [chapter 10].
- [24] Kim TY, Coi HJ, Cha SJ, Choi HK. Study on texture analysis of renal cell carcinoma nuclei based on the Fuhrman grading system. *Proc. IEEE Workshop Enterprise Networking Computing in Healthcare Industry*; 2005.
- [25] Gianazza E, Chinello C, Mainini V, Cazzaniga M, Squeo V, Albo G, et al. Alterations of the serum peptidome in renal cell carcinoma discriminating benign malignant kidney tumors. *J Proteomics* 2012;76:125–40.
- [26] Guyon I, Elisseeff A. An introduction to variable and feature selection. *J Mach Learn Res* 2003;3:1157–82.
- [27] Hall M. Correlation-based feature selection for discrete and numeric class machine learning. *Proc. 17th Intern. Conf. Machine Learning*. San Francisco: Morgan Kaufmann Publishers; 2000. p. 359–66.
- [28] Liu H, Yu L. Feature selection for high-dimensional data: A fast correlation-based filter solution. *Proc. 20th Intern. Conf. Machine Learning (ICML-03)*; 2003. pp. 856–63.
- [29] Michalewicz Z. *Genetic Algorithms + Data Structures = Evolution Programs*. Berlin: Springer; 1996.
- [30] Breiman L. Random forests. *Machine Learning* 2001;45:5–32.
- [31] Kuncheva L. *Combining pattern classifiers: methods and algorithms*. New York: Wiley; 2004.
- [32] Daliri MR. Combining extreme learning machines using support vector machines for breast tissue classification. *Comput Methods Biomech Biomed Eng* 2015;18(2):185–91.
- [33] Scholkopf B, Smola A. *Learning with Kernels*. Cambridge: MIT Press; 2002.